

Wideband Circularly Polarized Cross Bowtie Dipole Antenna with Axial-Ratio Bandwidth Enhancement

Dan Wu^{1, 2, *}, Zhi-Ya Zhang^{1, 2}, Luyang Ji^{1, 2}, Long Yang^{1, 2},
Guang Fu^{1, 2}, and Xiaowei Shi^{1, 2}

Abstract—A wideband circularly polarized (CP) cross-dipole antenna is proposed for wireless applications. In this design, four parasitic square patches are utilized around the radiation patch to enhance the Axial-ratio (AR) bandwidth. By employing the bowtie-shape dipoles, the proposed antenna can achieve a wide impedance bandwidth. Meanwhile, by integrating with a curved-delay line which provides a 90° phase difference, the proposed antenna can radiate a CP pattern. A prototype is calculated, fabricated, and measured. Good agreement between the simulated and measured results is achieved. The measured results show an impedance bandwidth for VSWR ≤ 2 of 47.73% (1.93–3.14 GHz) and a 3-dB AR bandwidth of 42.8% (2.00–3.09 GHz).

1. INTRODUCTION

Circularly polarized (CP) antennas have gained increasing attention in wireless systems such as satellite communication [1], global positioning system (GPS) [2], and radio frequency identification (RFID) [3] due to their great ability in anti-interference, better mobility, and multipath suppression [4]. Recently, many CP antennas are reported with different contributions, especially on the enhancement of the bandwidth [5–7]. Cross-dipole antenna is a conventional approach to achieve CP radiation owing to its advantages of relatively lower cost, lighter weight, and simpler structure. The initial realization of the cross-dipole antenna is achieved by employing two crossed dipoles with different lengths, which ensures the two orthogonal fields with equal amplitude and 90° phase difference [8]. However, the restriction associated with the conventional cross-dipole antenna is the narrow impedance and AR bandwidths. For wideband operation, several approaches have been proposed. A crossed bowtie dipole antenna with impedance bandwidth of 32% and AR bandwidth of 7.3% is proposed in [9]. By employing a sequentially rotated configuration, the cross-dipole antenna in [10] achieves a 30.7% impedance bandwidth and a 15.6% AR bandwidth, respectively. Though these aforementioned cross-dipole antennas can achieve wide impedance bandwidths, their AR bandwidths are narrow. The cross-dipole antenna with wide open ends in [11] and the cavity-backed detached crossed dipole in [12] can both realize broadband CP properties. The 3-dB AR bandwidths of 27% and 30% are realized in [11] and [12], respectively. In [13] and [14], extra resonances are realized by introducing half-wavelength parasitic resonators, which can generate a new minimum AR point. In [13], the antenna is loaded with a magneto-electric dipole to produce the wideband, and it has the AR bandwidth of 26.8%. The printed crossed dipole with a 3-dB AR bandwidth of 28.6% can be achieved by using four parasitic loops in [14]. However, antennas with the half-wavelength parasitic resonators have relatively large sizes. Moreover, the 3 dB AR bandwidths of the cross-dipole antennas in [11–14] range from 26.8% to 30% may not satisfy the requirements for modern wideband communication systems.

Received 15 January 2017, Accepted 22 February 2017, Scheduled 2 March 2017

* Corresponding author: Dan Wu (wudan44552@163.com).

¹ Science and Technology on Antenna and Microwave Laboratory, Xidian University, Xi'an, Shanxi 710071, China. ² School of Electronic Engineering, Xidian University, Xi'an, Shaanxi 710071, P. R. China.

In this paper, a CP cross-dipole antenna is proposed, which has a wide AR bandwidth by employing four parasitic square patches. The two crossed dipole elements are designed as a shape of bowtie, which contributes to achieving a wide impedance bandwidth. In order to generate a CP radiation, a curved-delay line is employed. Four parasitic square patches around the cross-dipole can effectively suppress the cross-polarization and enhance the co-polarization at high frequencies. This way, the proposed antenna can realize the AR bandwidth enhancement. The AR bandwidth can be enlarged from 9.3% of the structure without parasitic patch to 42.8%. The antenna shows a right-hand circularly polarized radiation with the center frequency of 2.5 GHz and its average gain within the operating bandwidth is around 6.6 dBic.

2. ANTENNA DESIGN AND PARAMETRIC DISCUSSION

The configuration of the proposed cross-dipole antenna is shown in Fig. 1. The proposed antenna is fabricated on a substrate with a thickness of 1.6 mm, permittivity of 4.4, and loss tangent of 0.02. The proposed antenna consists of five parts: two pairs of bowtie dipoles, a curved-delay line, four parasitic square patches, a ground and a coaxial line. The bowtie dipole has a wider impedance bandwidth than the ordinary cross-dipole in [10]. In order to achieve a broad impedance bandwidth, two pairs of bowtie dipoles are employed in the proposed antenna. Each pair is formed by two right-angled triangles. The dipoles are designed on both sides of the substrate. A curved-delay line is used to connect the two bowtie dipoles which can generate a 90° phase difference. Four parasitic square patches are printed on the same layer of the substrate with the corresponding dipole to realize a wide CP bandwidth as shown in Fig. 1. The proposed antenna is located a quarter-wavelength away from a square ground. The antenna is center-fed by a 50 Ohm coaxial line. The dipole located at the top side of the substrate is fed with the inner core of the coaxial cable through the etched hole shown in Fig. 1(a). The other dipole is connected to the outer conductor of the coaxial cable. The details of the antenna are as follows: $L = 70$ mm, $L_1 = 24$ mm, $L_2 = 22.38$ mm, $L_3 = 31.6$ mm, $W_1 = 20.55$ mm, $W_2 = 3.5$ mm, $W_3 = 7$ mm, $W_4 = 5$ mm, $W_5 = 2.5$ mm, $d = 15.61$ mm, $m = 1.92$ mm, $r = 5.9$ mm, $h = 1.6$ mm and $H = 31$ mm.

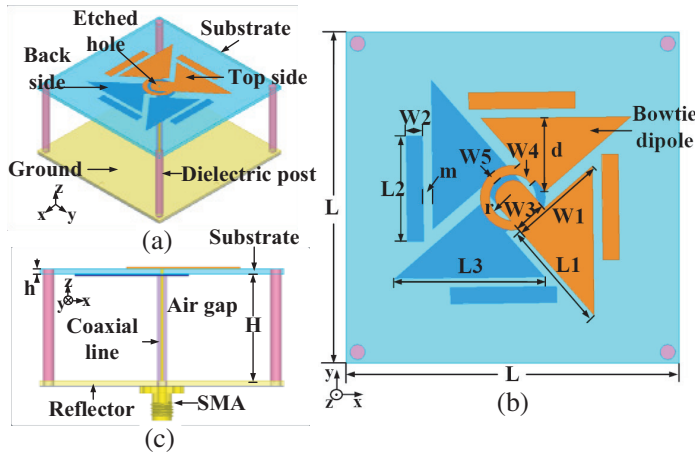


Figure 1. Geometrical configuration of the proposed antenna. (a) Perspective view, (b) top view, and (c) side view of the antenna.

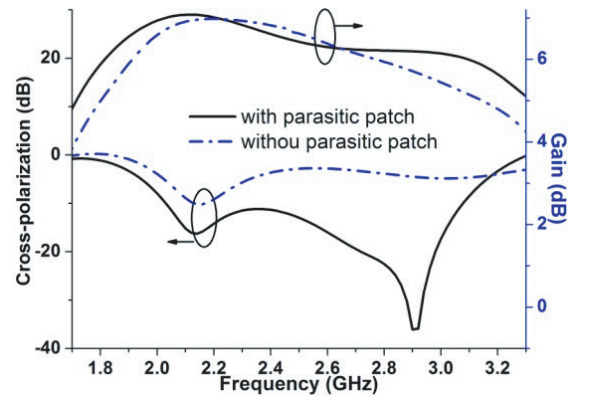


Figure 2. Simulated cross-polarization and gains variation with or without parasitic patch.

Though many conventional cross-dipole antennas have wide impedance bandwidth, their AR bandwidths are narrow. The antennas without parasitic patch can only perform a single minimum AR point well. To improve the AR bandwidth, four parasitic square patches with the length of a half-wavelength in the medium at high frequencies are placed in parallel around the bowties. The operating frequency of the four parasitic patches is controlled by the length of L_2 . To better illustrate the effect of the parasitic square patches on the AR property, a comparison between the bowties with and without

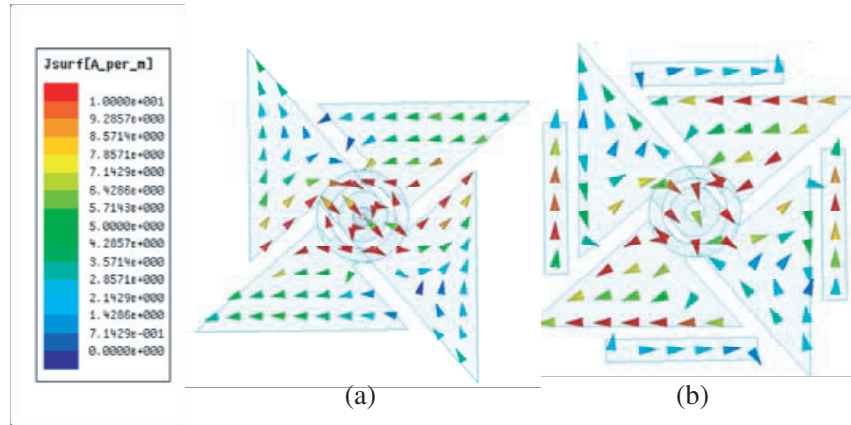


Figure 3. Simulated current distribution of the proposed antenna with or without parasitic patch at 2.9 GHz. (a) Without parasitic patch. (b) With parasitic patch.

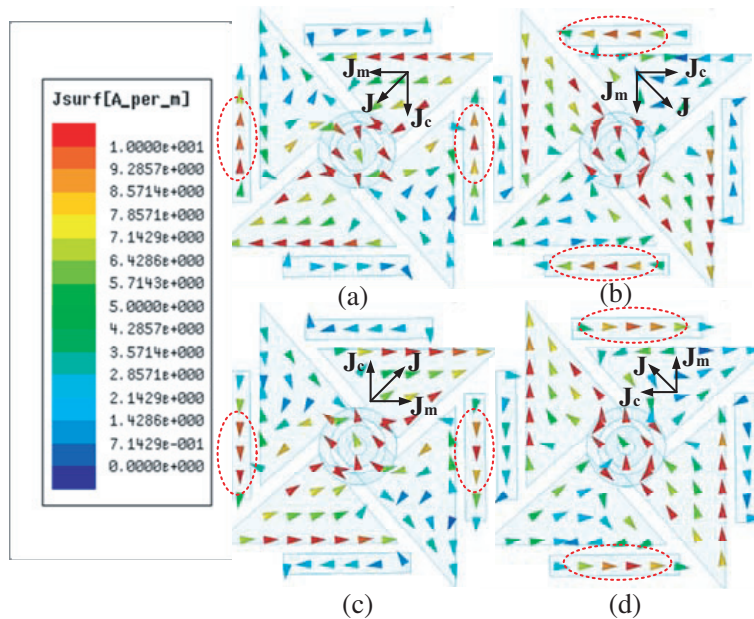


Figure 4. Current distribution of the proposed antenna at 2.9 GHz for different values of the phase angle. (a) 0°. (b) 90°. (c) 180°. (d) 270°.

parasitic patch is made. As shown in Fig. 2, the difference between the co- and cross-polarizations of the bowties without parasitic patch cannot meet the 3-dB AR requirement at high frequencies. On the other hand, the cross-polarization can be suppressed and the co-polarization enhanced at high frequencies when parasitic patches are employed, thus, the AR bandwidth can be improved.

As shown in Fig. 3, at high frequencies the bowties without parasitic patch radiate mainly near their centers. On the other hand, the current distributions can be changed owing to the coupling between the bowties and the four parasitic square patches. Comparing the current distributions between the bowties with and without the four parasitic patches, it can be found that the current distributions of the antenna with parasitic patch are mainly concentrated on the center and end of the bowties. The length of the current path at the end of the bowties is the same as that of the parasitic patches, which is approximately a half-wavelength in the medium at high frequencies. Hence, at high frequencies the antenna with parasitic patch radiates from not only the center region, but also the end region.

In Fig. 4, the surface current distributions of the proposed antenna at 2.9 GHz are presented to explain the improvement of the AR bandwidth. Note that J_m represents the current vector of the

co-polarization, while J_c represents the current vector of the cross-polarization at different time of a period. The current vector (J) at the center of the bowties in the figure can be decomposed into J_m and J_c . It can be seen that the current directions on the parasitic patches marked in the figure are opposite to the direction of J_c , and the magnitudes of the current on the parasitic patches marked in the figure are nearly the same as the that of J_c . Thus, the cross-polarization can be effectively suppressed at high frequencies. The current directions on the other parasitic patches are the same as the directions of J_m . The four parasitic square patches mainly function at high frequencies, since the length of that is a half-wavelength in the medium at high frequencies. Moreover, the current directions J_m at the end of the bowties are the same as the direction of J_m , which can enhance the amplitude of J_m . Compared with the antenna without parasitic patch, the cross-polarizations are suppressed, and the gains are enhanced from 2.7 to 3.2 GHz, as shown in Fig. 2. Hence, the AR bandwidth can be improved at high frequencies by introducing the four parasitic square patches.

To evaluate the effect of the parasitic patch parameters on antenna performance, several parameters are discussed below. Fig. 5 shows the variation of AR with different $W2$. When $W2 = 0$ mm, equivalent to the case without parasitic patches, only a single minimum AR point performs well. When $W2$ increases, the CP performance is improved at high frequencies. As $W2$ varies from 3 to 4 mm, the impedance bandwidths change slightly. The optimal result is achieved when $W2 = 3.5$ mm. When $W2$ is fixed, the value of $L2$ has a significant effect both on the AR and impedance bandwidths. Owing to the coupling between the bowties and the parasitic patches, the proposed antenna operates both at the center and the end of bowties at high frequencies. The length of the current path at the end of the bowties can be influenced by the length of the parasitic patches. Hence, the operating frequency decreases with the increase of the length ($L2$) of the parasitic patches at high frequencies, as shown in Fig. 6. The minimum AR point at high frequencies moves to the lower frequencies with the increase of $L2$. The achieved AR bandwidth is 42.8% when $L2$ is equal to 22.38 mm. The analysis above shows that the parameters of the parasitic patches mainly influence the performance of the proposed antenna at high frequencies. By appropriately choosing the values of $W2$ and $L2$, good impedance and AR bandwidths can be achieved.

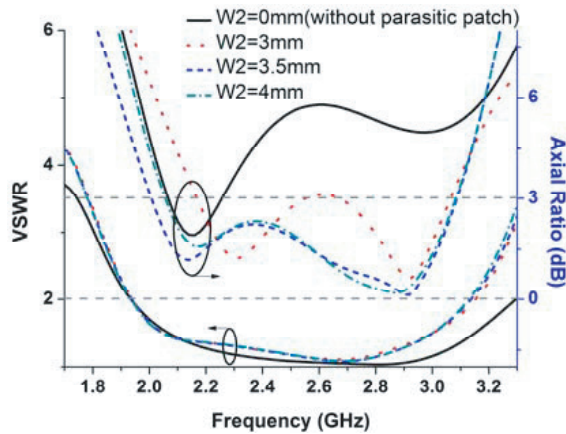


Figure 5. VSWRs and ARs of the proposed antenna with different $W2$.

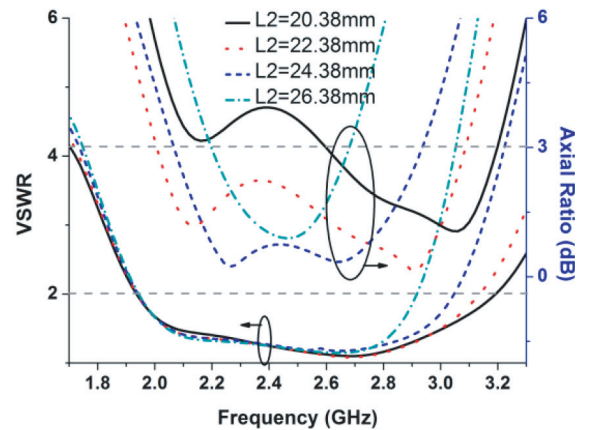


Figure 6. VSWRs and ARs of the proposed antenna with different $L2$.

3. EXPERIMENTAL RESULTS

As shown in Fig. 7, a prototype is designed, fabricated and measured. The measurements are implemented using Agilent E8363B network analyzer and an anechoic chamber. In order to keep the radiation pattern stable, a series of magnetic beads are used to prevent the surface current on the feeding cables. The measured and simulated VSWRs of the experimental prototype are presented in Fig. 8. The measured impedance bandwidth for $VSWR \leq 2$ is about 44.6% ranging from 1.95 GHz to 3.07 GHz. The results of the simulation and measurement agree well with each other. A comparison

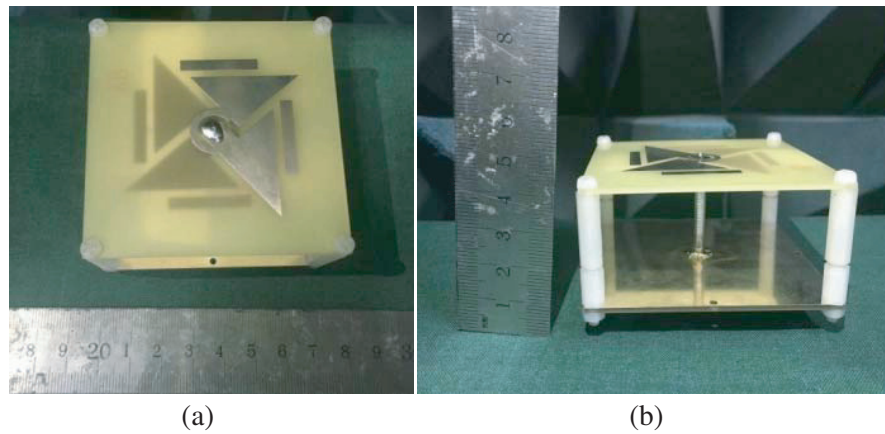


Figure 7. Photograph of the fabricated antenna. (a) Top view. (b) Side view.

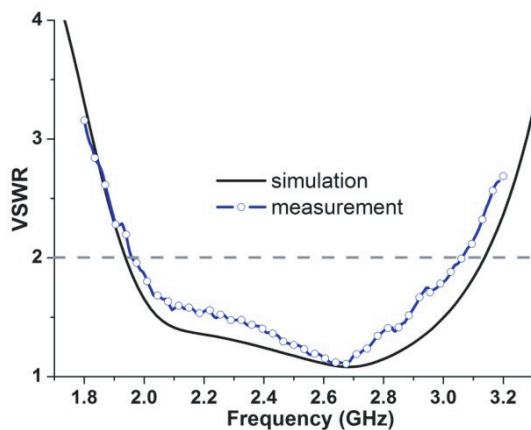


Figure 8. Measured and simulated VSWR of the proposed antenna.

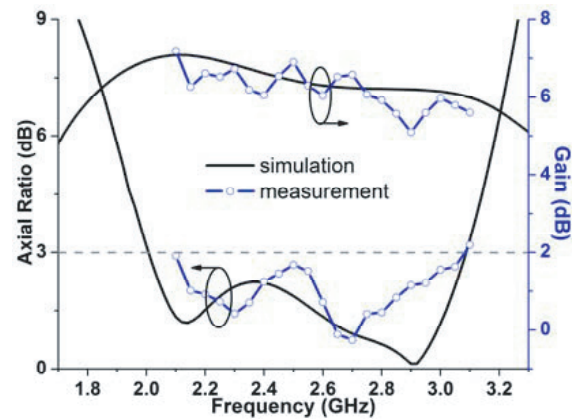


Figure 9. Measured and simulated ARs and gains of the proposed antenna.

between the measured and simulated AR bandwidths is shown in Fig. 9, where the measured 3-dB AR bandwidth starts from 2.08 to 3.08 GHz with a fractional bandwidth of 38.76%. It can be found that the simulation and measurement results are well corresponded with each other in AR characteristics. As illustrated in Fig. 9, the measured gains of the antenna in the direction of $\theta = 0^\circ$, $\varphi = 0^\circ$ are higher than 5.1 dBic across the operating frequency band with the peak gain of 7.2 dBic at 2.1 GHz.

Figure 10 shows the measured and simulated radiation patterns of the proposed antenna in the XOZ plane and YOZ plane, respectively, at 2.1, 2.5 and 3 GHz. The results indicate that the co-polarization is right-hand circularly polarized (RHCP), and the cross-polarization is left-hand circularly polarized (LHCP). It can be seen that the difference between the co- and cross-polarization levels is more than 15 dB at 2.1, 2.5 and 3 GHz, which can meet the 3-dB AR requirement. The 3-dB beamwidth is around 80° , and the measurements are well matched with the simulations in the main lobe. The measurements show that the proposed antenna has stable radiation patterns in both the XOZ and YOZ planes across the operating frequency band.

A comparison of the CP radiation performance is made between the proposed antenna and the reported cross-dipole antennas in references, as shown in Table 1. We find that the wide impedance bandwidth can be realized in [9, 10], and the wide AR bandwidth can be achieved in [11–14]. However, the AR bandwidth of the antennas proposed in [9–14] range from 7.3% to 30% may not satisfy the requirements for modern wideband communication systems. In general, the presented antenna has a better AR bandwidth.

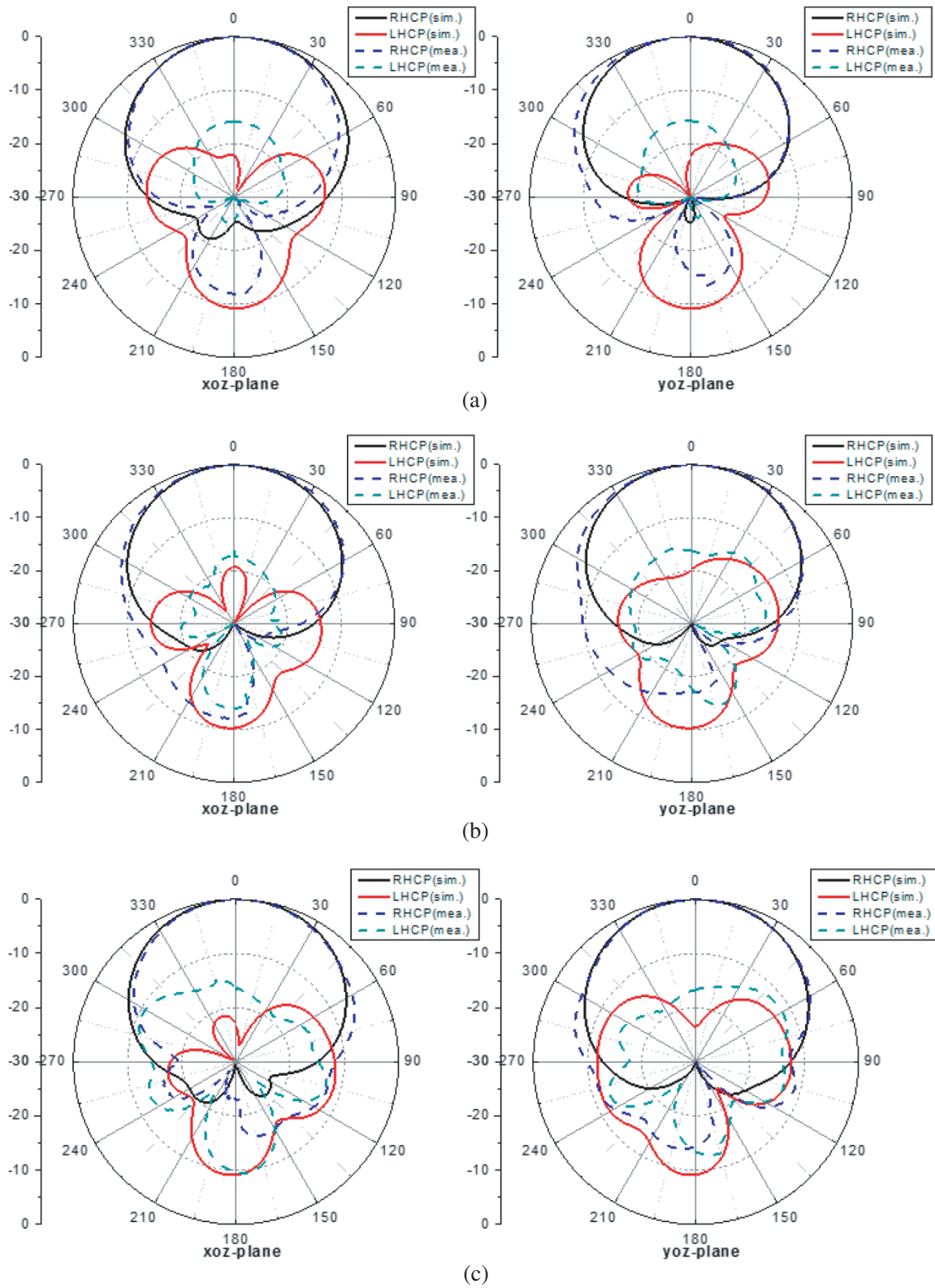


Figure 10. Radiation patterns of the antenna. (a) 2.1 GHz. (b) 2.5 GHz. (c) 3 GHz.

Table 1. Performance of cross-dipole antennas.

Antenna	Bandwidth (VSWR ≤ 2) (%)	3 dB AR Bandwidth (%)	Gain (dBic)	Size (λ_0^3)
Proposed	47.73	42.8	7.1	0.58 * 0.58 * 0.26
Ref. [9]	32	7.3	6	1.1 * 1.1 * 0.38
Ref. [10]	30.7	15.6	7.5	0.92 * 0.92 * 0.21
Ref. [11]	50.2	27	6.8	0.45 * 0.45 * 0.24
Ref. [12]	30	30	12.4	1.56 * 1.56 * 0.24
Ref. [13]	44.6	26.8	8	0.7 * 0.7 * 0.2
Ref. [14]	38.2	28.6	8.3	1 * 1 * 0.23

4. CONCLUSION

In this paper, a printed cross-dipole with four parasitic square patches is proposed for a broad AR bandwidth. Since the two crossed dipole elements are designed as a shape of bowtie, a wide impedance bandwidth can be obtained. To generate an orthogonal phase difference, the two bowtie dipoles are connected by a curved-delay line. Particularly, it has been demonstrated that at high frequencies the cross-polarization can be suppressed, and the co-polarization can be enhanced by introducing the four parasitic square patches. Hence, a broadband CP performance can be achieved. The AR bandwidths of the cross-dipole antenna with or without parasitic patches are 42.8% and 9.3%, respectively. Measurements show that the proposed antenna can operate in a frequency band from 2.07 to 3.07 GHz for both AR ≤ 3 dB and VSWR ≤ 2 , while an average gain of 6.2 dBi is realized. The final antenna shows the advantages of wide impedance and AR bandwidths, stable radiation patterns, simple structure and low cost. With these outstanding features, the proposed antenna can be a good candidate for modern wireless systems.

REFERENCES

1. Arnieri, E., L. Boccia, G. Amendola, and G. D. Massa, "A compact high gain antenna for small satellite applications," *IEEE Trans. Antennas Propag.*, Vol. 55, No. 2, 277–282, Feb. 2007.
2. Son, W. I. and W. G. Lim, "Design of compact quadruple inverted-F antenna with circular polarization for GPS receiver," *IEEE Trans. Antennas Propag.*, Vol. 58, No. 5, 1503–1510, May 2010.
3. Nasimuddin, Z., N. Chen, and X. Qing, "Asymmetric-circular shaped slotted microstrip antennas for circular polarization and RFID applications," *IEEE Trans. Antennas Propag.*, Vol. 58, No. 12, 3821–3828, Dec. 2010.
4. Bian, L., Y. X. Guo, L. C. Ong, and X. Q. Shi, "Wideband circularly polarized patch antenna," *IEEE Trans. Antennas Propag.*, Vol. 54, No. 9, 2682–2686, Sep. 2006.
5. Zou, M. and J. Pan, "A wideband circularly polarized rectangular dielectric resonator antenna excited by an archimedean spiral slot," *IEEE Antennas Wireless Propag. Lett.*, Vol. 13, 446–449, Oct. 2015.
6. Zhang, C. and X. Liang, "A broadband dual circularly polarized patch antenna with wide beamwidth," *IEEE Antennas Wireless Propag. Lett.*, Vol. 13, 1457–1460, Jul. 2014.
7. Cai, Y.-M. and K. Li, "Broadband circularly polarized printed antenna with branched microstrip feed," *IEEE Antennas Wireless Propag. Lett.*, Vol. 13, 674–677, Mar. 2014.
8. Bolster, M. F., "A new type of circular polarizer using crossed dipoles," *IRE Trans. Microw. Theory Tech.*, Vol. 9, No. 5, 385–388, Sep. 1961.

9. Yang, D. and H.-C. Yang, "A novel circularly polarized bowtie antenna for inmarsat communications," *IEEE Antennas and Propagation Magazine*, Vol. 54, No. 4, 317–325, Aug. 2012.
10. Baik, J.-W., K.-J. Lee, W.-S. Yoon, T.-H. Lee, and Y.-S. Kim, "Circularly polarized printed crossed dipole antennas with broadband axial ratio," *Electron. Lett.*, Vol. 44, No. 13, 785–786, Jun. 2008.
11. He, Y., W. He, and H. Wong, "A wideband circularly polarized cross-dipole antenna," *IEEE Antennas Wireless Propag. Lett.*, Vol. 13, 67–70, Jan. 2014.
12. Bai, X. and S.-W. Qu, "Ka-band cavity-backed detached crossed dipoles for circular polarization," *IEEE Trans. Antennas Propag.*, Vol. 62, No. 12, 5944–5950, Dec. 2014.
13. Ta, S. X. and I. Park, "Crossed dipole loaded with magneto-electric dipole for wideband and wide-beam," *IEEE Antennas Wireless Propag. Lett.*, Vol. 14, 358–361, Feb. 2015.
14. Baik, J.-W. and T.-H. Lee, "Broadband circularly polarized crossed dipole with parasitic loop resonators and its arrays," *IEEE Trans. Antennas Propag.*, Vol. 59, No. 1, 80–88, Jan. 2011.